AMERICAN JOURNAL of PHYSICS

A daylight experiment for teaching stellar interferometry

M. A. Illarramendi, R. Hueso, J. Zubia, G. Aldabaldetreku, G. Durana, and A. Sánchez-Lavega

Citation: American Journal of Physics **82**, 649 (2014); doi: 10.1119/1.4869280
View online: http://dx.doi.org/10.1119/1.4869280
View Table of Contents: http://scitation.aip.org/content/aapt/journal/ajp/82/7?ver=pdfcov
Published by the American Association of Physics Teachers

A daylight experiment for teaching stellar interferometry

M. A. Illarramendi, R. Hueso, J. Zubia, G. Aldabaldetreku, G. Durana, and A. Sánchez-Lavega
University of the Basque Country UPV/EHU, Escuela Técnica Superior de Ingeniería Bilbao, Alda. Urquijo s/n, E-48013 Bilbao, Spain

(Received 30 July 2012; accepted 11 March 2014)

We discuss the design of a simple experiment that reproduces the operation of the Michelson stellar interferometer. The emission of stellar sources has been simulated using light emerging from circular end-faces of step-index polymer optical fibers and from diffuse reflections of laser beams. Interference fringes have been acquired using a digital camera, coupled to a telescope obscured by a double aperture lid. The experiment is analogous to the classical determination of stellar sizes by Michelson and can be used during the day. Using this experimental set-up, we can determine the size of extended sources, located at a distance of about 75 m from our telescope, with errors less than 25%.
[http://dx.doi.org/10.1119/1.4869280]

I. INTRODUCTION

The major challenges in observational astronomy are the detection of faint objects and improvements in spatial resolution. Theoretically, both problems can be addressed by increasing the size of the telescope objective, thus increasing the collecting area for photons and, at the same time, reducing the size of the Airy disk that limits the resolution. For most ground-based telescopes, the turbulent motion of the Earth's atmosphere degrades the resolution of an image and high-resolution observations require either the use of adaptive optics instruments to correct for the effects of turbulence or lucky imaging detectors to effectively freeze the distortions created by the atmospheric turbulence.

Most stars are so far away that even space telescopes, such as the Hubble Space Telescope with a diameter of 2 m, or the most powerful ground-based telescopes, such as the Grantecan in Spain with a diameter of 10.2 m, are unable to directly resolve their disks. The closest giant stars, such as α Orionis (Betelgeuse) with a size of about 630 solar radii, subtend a small angle of about 50 milliarcseconds (mas). Aside from the Sun, this is one of the few stars whose size has been measured at visible wavelengths. Initial measurements of its size were carried out using the principles of interferometry, a technique that combines the radiation gathered by two or more telescopes.[1,2] Albert A. Michelson and Francis Pease were the first to measure the size of Betelgeuse in 1920 using a novel stellar interferometer—the "Michelson interferometer"—mounted on the 2.5 m diameter Hooker telescope at Mount Wilson Observatory.[3]

Interferometry is a valuable tool in the study of stellar evolution as it allows the measurement of the basic parameters of stars, such as mass, radius, and temperature that require high-resolution data. Interferometry has provided high angular resolution at radio wavelengths,[4] and even higher resolutions are achievable with optical interferometers that operate at near-infrared (1–11 μm) and visible (0.5–0.8 μm) wavelengths. Since the experiment by Michelson and Pease, different interferometer types have been used to improve the resolution at optical and infrared wavelengths, such as the correlation or intensity interferometer by Hanbury Brown[5,6] and the speckle interferometry method developed by Labeyrie.[7] The path to higher resolution requires telescopes operating at short wavelengths. Some examples of optical interferometers are the very large telescope interferometer (VLTI),[8] the CHARA array,[9] and the navy precision optical interferometer (NPOI).[10]

The introduction of the subject of stellar interferometry to undergraduate and graduate students is not easy and has hardly been developed. The subject is largely ignored in most astronomy textbooks[11] and only the classic Michelson interferometer is acknowledged.[12] Although Michelson's method for determining the angular dimensions of astronomical objects is described in classic textbooks of optics,[1,2] little has been written concerning experimental activities related to the optical principles of stellar interferometry.[13–15] It is worth mentioning the experiment for undergraduate students reported recently by Sharpe and Collins,[13] where the effect of the source size on optical coherence is analyzed. Although these types of experiments can be useful to show how optical coherence can be used in astronomy, they suffer from a lack of connection with the courses they are designed to support. For instance, in these experiments, telescopes are not used or the light source is placed close to the telescope. To overcome those difficulties and in the spirit of introducing the subject in a practical way, we have developed an experimental method that allows direct measurement of the size of distant extended sources during the day. Our experiment is also suitable for graduate courses in astronomy, optics, or space science.[16] The experiment is based on the optical principles of the Michelson stellar interferometer, uses simple equipment that is available in most astronomy and optics departments, and can be integrated into existing courses with close interaction between theory and experiment.

II. FUNDAMENTALS

The optical fundamentals of the Michelson stellar interferometer are based on those of the familiar Young's double-slit experiment. In this classic experiment, monochromatic light from a source is used to illuminate two slits. The light emerging from both slits interfere and form interference fringes on the viewing screen. In stellar interferometry, we superimpose two separate beams of the light emitted from a distant star on a telescope. This can be done by placing a lid with two circular apertures, with variable separation, in front of the objective of the telescope. The image of the source is formed at the focal plane of the telescope and, if the apertures on the lid are close enough, it appears striped because of the interference between the light beams. The quality of the interference fringes in the image can be described quantitatively in terms of the fringe visibility V, which is defined as

$$V = \frac{I_{\max} - I_{\min}}{I_{\max} + I_{\min}}, \tag{1}$$

where $I_{\max}$ and $I_{\min}$ are the maximum and minimum intensities of the interference fringes, respectively. The fringe visibility is a measure of the degree of coherence of the light coming from a spatially incoherent source across the double aperture lid.[1,2,17] For our analysis, we assume that the light reaching the aperture of the telescope from such a source is spatially coherent over an area that increases quadratically with the distance from the source.[18] This area is called the coherence area. The connection between Young's double-slit experiment, the Michelson stellar interferometer, and the partial coherence theory was established in the well-known experimental study of two-beam interference with partially coherent light carried out by Thompson and Wolf many years ago.[19]

If we take the simplest model to describe the emission of a star—a circular, uniform, and spatially incoherent source emitting quasi-monochromatic light—the fringe visibility is given by Refs. 1 and 2,

$$V = 2\left|\frac{J_1(\pi a d/L\lambda)}{(\pi a d/L\lambda)}\right|, \tag{2}$$

where J_1 is the first-order Bessel function of the first kind, a the (linear) diameter of the source, L the distance between the source and the double-aperture system, d the distance between the two apertures or pinholes, and λ the wavelength of the light. According to Eq. (2), the visibility V decreases steadily from a value of unity when $\pi a d/L\lambda = 0$ to a value of zero when $\pi a d/L\lambda = 1.22\pi$. If the visibility V of the fringes is measured as a function of the pinhole separation d, the diameter of the source a can be determined if the distance L and the wavelength λ are known. The easiest procedure to determine the diameter of the source is to determine the lowest value of d for which the interference fringes disappear. This happens when $d = 1.22\lambda L/a$. A more accurate value of the source size can be obtained by fitting the measured visibility to Eq. (2).

III. EXPERIMENTAL SET-UP AND PROCEDURE

Figure 1 shows a schematic of the experimental setup used in this work. The distant source is a circular end-face of a 2-m-long step-index polymer optical fiber (SI-POF) coupled to a laser, as shown in Fig. 1(a). The polymer optical fiber has a large core diameter ($\approx$1 mm) and its light gathering (or emitting) capacity, a measure given by its numerical aperture (NA), is 0.5. Because SI-POFs are, in general, highly multimode, the 2-m-long fiber used in this set-up is sufficient to ensure that the conditions of a uniform and spatially incoherent source are met at the output surface of the fiber.[20,21] Equation (2) can be used to describe the variation of fringe visibility with pinhole separation. The SMA fiber connectors allow us to connect fiber-beam expanders and collimators. This allows us to increase the size of the circular source and, at the same time, decrease the numerical aperture of the output light. Additional phase terms introduced by the fiber beam expanders do not alter the values of the interference intensity at the double aperture lid.

If the assembly of the source with the polymer fiber proves difficult, a simpler source can be used to carry out the experiment. This source uses diffuse reflection of a circular laser beam or Light Emitting Diodes (LEDs). Diffuse reflection can be obtained by shining the laser beam on a rough surface, such as a cork board. We have assumed that the reflected laser beam is uniform and that the spatial coherence of the laser light is lost in the diffuse reflection process. The source size is measured by putting white paper on the cork board and drawing the perimeter of the laser spot. In our experiments, we use a commercial laser diode (QIOPTIQ), emitting approximately 5 mW at 635 nm, and beam expanders suitable for this wavelength (Thorlabs SMA fixed aspheric lens fiber packages).

The light source equipment is placed inside a room on the roof of one building of our institution and the emission is observed with a reflector telescope in a laboratory on the top floor of another building. The path is shown in Fig. 1(b). Accurate values for the distance L between the source and

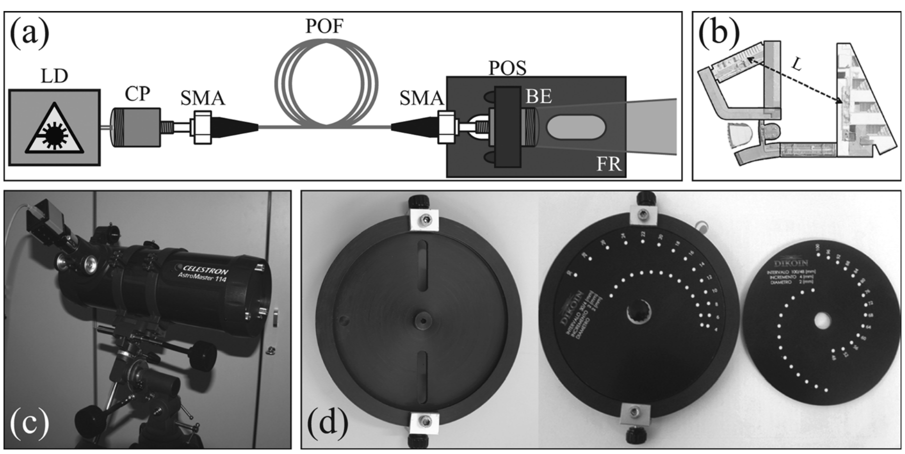

Fig. 1. (a) Experimental set-up of the extended source. LD: laser diode; CP: fiber coupler; SMA: SMA connector; POF: polymer optical fiber; POS: positioner; BE: beam expander; FR: flat rail. (b) Distance L between the extended source and the telescope on the map of our institution. (c) Reflector telescope with the coupled camera. (d) Internal slit and external revolving lids with circular apertures. The separation distances between the pinholes are indicated on the mask in millimeters; the distance is changed by turning the revolving lid.

the telescope are obtained using a global positioning system (GPS) device (Garmin GPSmap 76CSx). The location data of the source and the telescope are retrieved from the GPS in a latitude and longitude format and the distance between them is calculated using the haversine formula, which is accurate enough for our purpose.

Figure 1(c) shows the telescope used for the detection of the images. We use the AstroMaster 114 EQ Newtonian with a 114 mm aperture and focal distance of 1000 mm. Once the telescope is well focused, its aperture is blocked by a lid with two identical circular pinholes. To obtain a variable and measurable distance between both pinholes, we designed revolving lids, shown on the right-hand side in Fig. 1(d). Both lids have pairs of identical pinholes, separated by different distances. The pinholes all have a diameter of 2 mm and we can adjust the pinhole separation over a range between 4–100 mm by turning the external revolving lid. On the left-hand side of Fig. 1(d), the internal slit is shown, which allows light to pass through only one pair of pinholes at any given time.

The fringe pattern can be observed directly through an eyepiece and digital images can be acquired with a camera attached to the focal plane of the telescope. We use a DMK41AU02 commercial camera equipped with the Sony ICX205AL CCD chipset, extensively used by amateur astronomers.[22] This camera has a sensitivity of 0.05 lx, a dynamic range of 36 dB, and a pixel size of 4.65 μm.

The experiments are carried out on a cloudy day to avoid stray light that reduces the visual contrast and increases the noise in the measurements. The light in the room where the source is placed is turned off. Because the light source is placed a long distance away from the telescope, long exposures are required to obtain images of the fringes. Because our experiment is carried out during the day, there is an upper limit to the exposure time before the images become saturated due to stray light in the field of view. In the experiments with the polymer fiber source, we use 2 min exposures for each image, and in the experiment with the diffuse reflection source we use 4 min exposures. Images are digitized into 512 levels and processed by standard astronomical image processing software (PLIA).[23] The intensities I_{max} and I_{min} are measured by selecting the appropriate points on the fringes with a cursor; I_{max} is measured at the central brightest fringe and I_{min} is obtained from the average of two measurements acquired in the adjacent dark fringes (the difference between these values can be used to estimate the measurement uncertainties). Because the experiments are carried out during the day, the background brightness is determined using measurements outside the interference pattern and subtracted from all measured values. Each measurement uses the median value over a box of 3×3 pixels, centered at the position of the cursor, which minimizes the influence of sensor noise on the measured intensities.

IV. RESULTS

Figure 2 shows the fringe visibility as a function of the pinhole separation. These results are obtained using an emitting circular end face of a 2-m-long SI-POF with a beam expander. The diameter of the source is 3 mm and the numerical aperture of the output light is NA = 0.11 (at $\lambda = 635$ nm). The errors in the visibility values are estimated from the values of the diffuse background in the digital image and the pixel-to-pixel noise. As seen in Fig. 2, the fringe visibility diminishes as the pinhole separation increases. As the distance L increases, the coherence area of the light across the lid will be larger and a secondary visibility maximum can be detected at larger pinhole separations. Figure 3 shows the interference patterns and the relative brightness profiles of the images obtained at three different pinhole separations of $d = 4$, 12, and 20 mm. Note how the striped lines caused by the two-beam interference are modulated by the larger Airy pattern generated by the single circular aperture, and how the spatial frequency of the fringes increases as d increases. Fitting Eq. (2), with $L = 75 \pm 3$ m and $\lambda = 635 \pm 1$ nm, to the measured visibility distribution in Fig. 2, we deduce a source diameter of $a = 3.1 \pm 0.2$ mm. This diameter differs by 3% from the actual value.

A second experiment, not requiring an optical fiber, uses a laser beam reflected from an irregular surface. The diffuse reflection had a diameter of 3 ± 1 mm. Figure 4 shows the measured fringe visibility obtained using this setup. As before, the visibility decreases with increasing pinhole separation. However, due to the broader angular distribution of the diffuse reflected light, the intensity detected by the camera is much lower than in the previous experiment. Consequently, the dispersion is larger in this experiment compared to the first. A fit of Eq. (2), using $L = 78 \pm 3$ m and $\lambda = 635 \pm 1$ nm, to the measured visibility in Fig. 4 leads to a source diameter of $a = 2.3 \pm 0.2$ mm. The deviation from the actual size is 23%, much larger than the 3% obtained in the first experiment. The use of the diffuse reflection of a laser beam as a distant source requires more assumptions about the characteristics of the source to describe the emission and it provides lower intensities at the camera.

It should be noted that the CCD/telescope system can in practice resolve the size of the object in this set of experiments by direct observation (without any lid) because the maximum distance between the pinholes is smaller than the aperture of the telescope and the CCD pixel size is smaller than the 1.4″ limit of diffraction of the telescope. Thus, for a pixel size of 4.65 μm and a focal length of 1000 mm, the coverage of each pixel is 0.95″. This contrasts with the original Michelson and Pease measurements, which were obtained

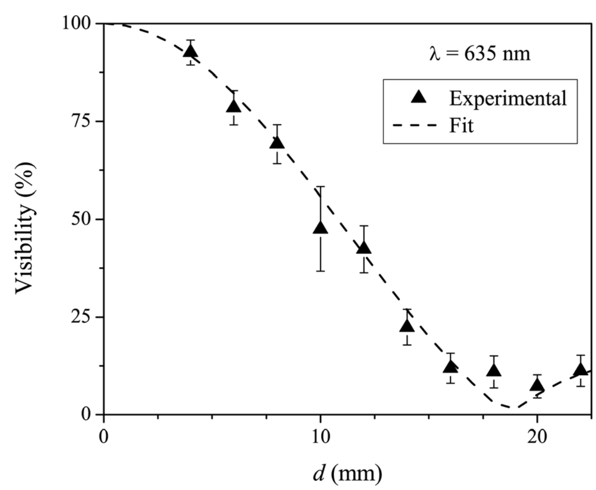

Fig. 2. The measured visibility as a function of the pinhole separation, obtained for a circular source placed at $L = 75$ m. The source is the end-face of a 2 m long SI-POF with a beam expander, with a diameter of 3 mm, emitting light at $\lambda = 635$ nm with NA = 0.11. The triangles show the measured visibilities obtained from the captured images. The dashed curve shows a fit to the data using Eq. (2).

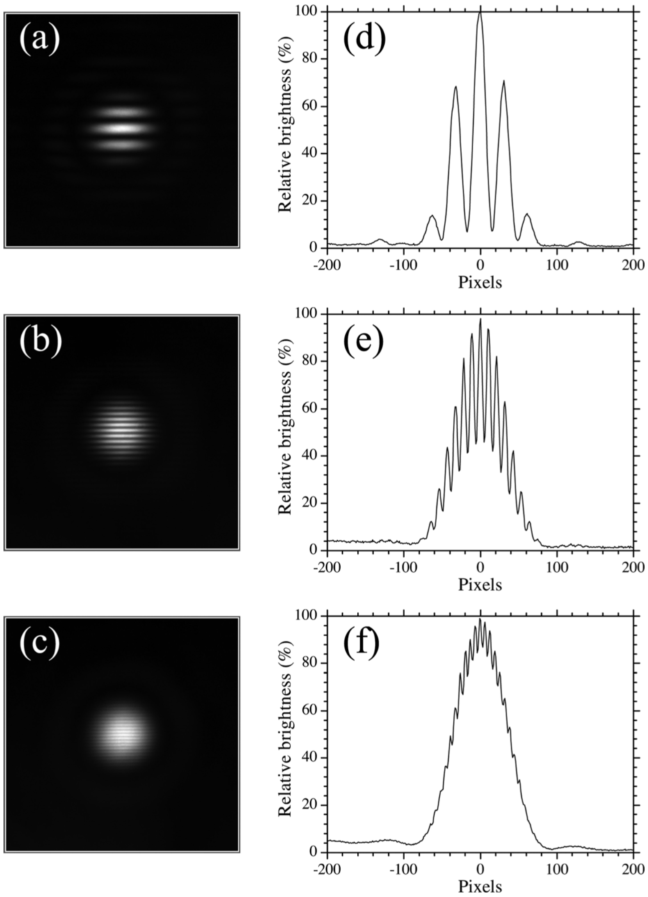

Fig. 3. Interference patterns formed by light from a circular source placed at $L = 75$ m with three pinhole separations: (a) $d = 4$ mm, (b) $d = 12$ mm, and (c) $d = 20$ mm. The source is the circular end-face of a 2 m long SI-POF with a beam expander, with a diameter of 3 mm, emitting light at $\lambda = 635$ nm with NA = 0.11. The relative brightness profiles of the images are also shown for the same pinhole separations: (d) $d = 4$ mm, (e) $d = 12$ mm, and (f) $d = 20$ mm.

using a system of external mobile mirrors that could be separated up to a distance of 6 m, providing a longer baseline for interferometry. Although the present exercise is a heuristic one, it serves to demonstrate the operation of the stellar interferometer using inexpensive equipment.

The experiment can be simplified for introductory laboratories if the camera is not used to measure the fringe visibility. In this case, the student would turn the external revolving lid to produce the minimum in the fringe visibility and then write down the corresponding pinhole separation. Using this separation distance, it is straightforward to calculate the diameter of the object. The experiment can also be modified by using a uniform rectangular source (this type of source can easily be obtained for the case of diffuse reflections of laser beams by inserting a cylindrical lens behind the laser). The visibility curves for this geometry are sinc functions.[2] The dimensions of the rectangular source can be obtained by determining the lowest values of the pinhole separation for which the interference fringes disappear at two perpendicular orientations of the internal slit. For advanced laboratory students who have been introduced to the theory of coherence, the experiment can be used to characterize sources with slightly more complex brightness distributions, such as a double "star" system, by measuring the visibility curves with multiple orientations of the internal slit.

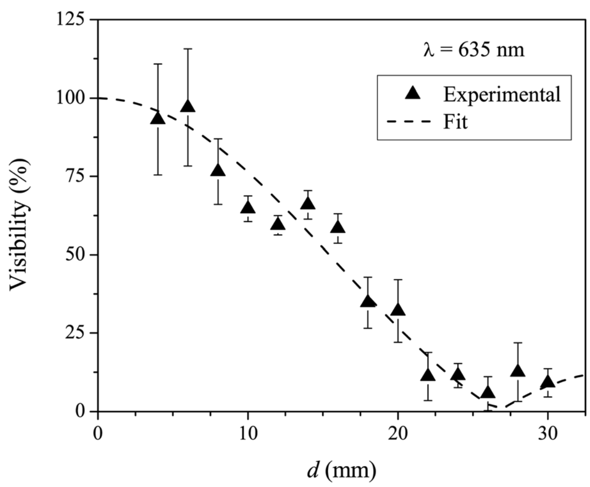

Fig. 4. The measured visibility as a function of the pinhole separation, obtained for a circular source at a distance of $L = 78$ m. The source is a diffuse reflection of a laser beam ($\lambda = 635$ nm), with a spot diameter of 3 mm. The triangles show the measured visibilities obtained from the captured images. The dashed curve shows a fit to the data using Eq. (2).

V. SUMMARY

We have designed an experiment to demonstrate the fundamentals of the Michelson stellar interferometer during the day. As our remote source we use the output surface of a multimode SI-POF coupled to a laser. This source produces an emission pattern that is similar to the emission pattern of stellar sources—circular, uniform, spatially incoherent, and quasi-monochromatic. The diffuse reflections of a circular laser beam can also be used as the distant source. It has been demonstrated that our method is able to measure the size of circular sources that are about 100 m away with an error of less than 25%. The measured source sizes and distances correspond to angular diameters on the order of 20″, a value comparable to the size of Mars (25″) and Saturn (20″), and smaller than Jupiter (45″) and Venus (53″). The use of a telescope, a digital camera, and image processing tools, makes this experiment very appropriate for astronomy, astrophysics, optics, and space-science students.

A possible extension of this experiment would be to measure the angular diameters of the planets in our solar system. Such an extension would require longer exposure times and could be done using a robotic telescope mount and a narrow-band filter for the camera. For instance, a telescope with a 20 cm aperture and an appropriate lid would be capable of measuring the sizes of all solar system planets. By increasing the aperture to 50 cm we could also measure the sizes of large satellites, such as Titan (0.7″), Ceres (0.6″), or Vesta (0.4″). Finally, this experiment could be adapted to introductory students if the size of the source were determined by measuring the lowest value of the pinhole separation for which the interference fringes disappear.

ACKNOWLEDGMENTS

This work has been supported by the institutions Diputación Foral de Bizkaia/Bizkaiko Foru Aldundia through the Aula Espazio Gela, Ministerio de Economía y Competividad under project TEC2012-37983-C03-01, Gobierno Vasco/Eusko Jaurlaritza under projects GIC07/156-IT-343-07, AIRHEM-II, SAI12/174, IT-343-07, IT-464-07, and AYA2009-10701 with

FEDER funds, and by the University of the Basque Country (UPV/EHU) through programs UFI11/16 and UFI11/55.

[1]E. Hecht and A. Zajac, *Optics*, 4th ed. (Addison-Wesley, Reading, MA, 2003).

[2]M. Born and E. Wolf, *Principles of Optics*, 7th ed. (Pergamon Press, London, 2002).

[3]A. A. Michelson and F. G. Pease, "Measurement of the diameter of alpha Orionis with the interferometer," Astrophys. J. **53**, 249–259 (1921).

[4]K. I. Kellermann and D. S. Heeschen, "Radio astronomy in the 1990s," Phys. Today **44**, 40–45 (1991).

[5]R. Hanbury Brown and R. Q. Twiss, "A test of a new type of stellar interferometer on Sirius," Nature **178**, 1046–1048 (1956).

[6]R. Hanbury Brown, "Measurement of stellar diameters," Annu. Rev. Astron. Astrophys. **6**, 13–38 (1968).

[7]A. Labeyrie, "Attainment of diffraction limited resolution in large telescopes by Fourier analysing speckle patterns in star images," Astron. Astrophys. **6**, 85–87 (1970).

[8]The Very Large Telescope Interferometer, <http://www.eso.org/sci/facilities/paranal/telescopes/vlti>.

[9]Center for High Angular Resolution Astronomy, <http://www.chara.gsu.edu/CHARA>.

[10]Navy Precision Optical Interferometer, <http://www.lowell.edu/npoi/index.php>.

[11]B. W. Carroll and D. A. Ostlie, *An Introduction to Modern Astrophysics* (Pearson Education, San Francisco, 2007).

[12]*Fundamental Astronomy*, edited by H. Karttunen, P. Kroger, H. Oja, M. Poutanen and K. J. Donner, 5th ed. (Springer-Verlag, Berlin, 2007).

[13]J. P. Sharpe and D. A. Collins, "Demonstration of optical spatial coherence using a variable width source," Am. J. Phys. **79**, 554–557 (2011).

[14]B. T. King and W. Tobin, "Charge-coupled device detection of two-beam interference with partially coherent light," Am. J. Phys. **62**, 133–137 (1994).

[15]D. Ambrosini, G. Schirripa Spagnolo, D. Paoletti, and S. Vicalvi, "High precision digital automated measurement of degree of coherence in the Thompson and Wolf experiment," Pure Appl. Opt. **7**, 933–939 (1998).

[16]Master in Space Science and Technology, <http://www.ehu.es/aula-espazio/english/master.html>.

[17]J. W. Goodman, *Statistical Optics* (John Wiley & Sons Inc., 2000).

[18]E. Wolf, *Introduction to the Theory of Coherence and Polarization of Light* (Cambridge U. P., 2007).

[19]B. J. Thompson and E. Wolf, "Two-beam interference with partially coherent light," JOSA **47**, 895–902 (1957).

[20]H. Yoshimura, T. Asakura, and N. Takai, "Spatial coherence properties of light from optical fibres," Opt. Quantum Electron. **24**, 631–646 (1992).

[21]M. Imai and Y. Ohtsuka, "Spatial coherence of laser light propagating in an optical fibre," Opt. Quantum Electron. **14**, 515–523 (1982).

[22]E. Grafton, "Get ultra sharp planetary images with your CCD camera," Sky and Telescope **106**(3), 125–128 (2003).

[23]R. Hueso, J. Legarreta, J. F. Rojas, J. Peralta, S. Pérez-Hoyos, T. del Río-Gazteluurrutia, and A. Sánchez-Lavega, "The planetary laboratory for image analysis (PLIA)," Adv. Space Res. **46**, 1120–1138 (2010).